Prognostic Significance of Cadherin-Based Adhesion Molecules in Cutaneous Malignant Melanoma

Gretchen M. Kreizenbeck,[1] Aaron J. Berger,[1] Antonio Subtil,[2] David L. Rimm,[1] and Bonnie E. Gould Rothberg[3]

Departments of [1]Pathology, [2]Dermatology, and [3]Epidemiology and Public Health, Yale University School of Medicine, New Haven, Connecticut

Abstract

Background: **The need for novel molecular prognostic markers that can supplement validated clinicopathologic correlates for cutaneous malignant melanoma is well recognized. Proteins that mediate the epithelial-mesenchymal transition, the process by which a cancer cell disengages from its parent tumor, are important candidates.**

Methods: **The prognostic relevance of E-cadherin, N-cadherin, and P-cadherin, calcium-dependent transmembrane glycoproteins that regulate cell-cell adhesion, and their adaptors, α-catenin, β-catenin, and p120-catenin, was evaluated on a cohort of 201 primary and 274 metastatic melanoma tumors using fluorescence-based immunohistochemical methods and Automated Quantitative Analysis of protein expression on digitally captured photomicrographs.**

Results: **Increasing levels of N-cadherin expression improved overall survival (log-rank = 7.31; $P = 0.03$) but did not retain significance following adjustment for established clinicopathologic correlates ($P = 0.50$). Higher levels of E-cadherin approached significance for favorable prognosis on both univariate ($P = 0.13$) and multivariable ($P = 0.10$) analyses. Hierarchical clustering of the composite profiles for all six markers identified four unique clusters that yielded differential overall survival (log-rank = 10.54; $P = 0.01$). Cluster 4, expressing high E-cadherin and N-cadherin levels, possessed the most favorable outcome and cluster 2, featuring low E-cadherin and α-catenin but modest N-cadherin, showed least favorable outcomes. Cluster 2 remained significant on multivariable analysis (hazard ratio, 3.29; 95% confidence interval, 1.50-7.19; $P = 0.003$).**

Conclusions: **Although none of the cadherin-based adhesion molecules were independently prognostic, multimarker profiles were significant. Similar to epithelial-derived tumors, loss of E-cadherin correlates with poor outcome. In contrast, for neural crest–derived cutaneous malignant melanoma, N-cadherin overexpression can be associated with either a successful epithelial-mesenchymal transition or a favorably differentiated tumor. Additional cadherin profiles are needed to discriminate these distinctive phenotypes.** (Cancer Epidemiol Biomarkers Prev 2008;17(4):949–58)

Introduction

Cutaneous malignant melanoma (CMM), with 59,400 new cases estimated in 2007, represents the sixth most common malignancy in the United States and a growing public health challenge (1). Although just over 80% of new melanomas will be localized to the skin where effective surgical resections will result in >90% 5-year survival, the remaining patients will be diagnosed with either regional (12%) or distant (4%) disease (1). Due to the refractoriness of melanoma to pharmacologic interventions, the majority of these patients will succumb to their disease. Because disease can recur even among individuals with localized lesions despite appropriate surgical procedures, identifying independent prognostic markers in addition to stage at diagnosis has been a priority. Presently, nine additional independent clinicopathologic prognostic markers for CMM have been identified [e.g., age at presentation, gender, Breslow thickness (mm), Clark level of invasion, lesion ulceration, tumor-infiltrating lymphocyte status, presence of microsatellite lesions, degree of vascular and/or lymphatic invasion, and quantity of mitotic figures] and have been used to establish clinically validated risk stratifications among melanoma patients (2, 3). Yet, in CMM (4, 5), as well as in other cancers (6, 7), the association of differential gene expression profiles with prognosis among histologically identical lesions has prompted the desire to enhance clinicopathologically derived prognostic models with molecular markers representative of the tumor subclasses. Efforts to improve CMM prognostic models have thus been focusing on identifying proteins whose differential expression can further refine prediction of CMM outcomes independently of the known clinical criteria.

The intimate relationship between CMM prognosis and the presence of metastatic foci has led to the investigation of whether genes involved in the regulation of the epithelial-mesenchymal transition (EMT) in melanocytes are useful independent prognostic markers of

Received 10/24/07; revised 1/10/08; accepted 1/15/08.

Grant support: NIH grant RO-1 CA 114277 (D.L. Rimm).

The costs of publication of this article were defrayed in part by the payment of page charges. This article must therefore be hereby marked *advertisement* in accordance with 18 U.S.C. Section 1734 solely to indicate this fact.

Requests for reprints: Bonnie E. Gould Rothberg, Department of Epidemiology and Public Health, Yale University School of Medicine, 60 College Street, New Haven, CT 06520-8034. Phone: 203-737-4205; Fax: 203-737-5089. E-mail: bonnie.gouldrothberg@yale.edu

doi:10.1158/1055-9965.EPI-07-2729

melanoma. EMT refers to the process in which an epithelial cell disengages from its parent tissue by losing mediators of homotypic and/or local heterotypic cell-cell interactions in exchange for morphology and adhesion marker profiles consistent with a mesenchymal cell and is regarded as the first necessary step for invasion and metastasis (8). This pathway is especially germane for melanoma because EMT recapitulates a pivotal phase of melanocytic development. Normal melanoblast precursors are derived from the neural crest. During embryogenesis, these cells undergo a first EMT to disengage from the neural crest and then subsequently migrate through the embryonic mesenchyme until they reach their terminal locations distributed throughout the dermal/epidermal junction where they subsequently undergo a reverse EMT to facilitate interactions with local keratinocytes. Melanocytic migration is one of the few appropriate, developmentally programmed EMTs documented in metazoan biology (9).

Among important mediators of the EMT are the cadherins, a family of calcium-dependent, transmembrane glycoproteins that regulate cell-cell adhesion, and the catenins, intracellular binding partners of the cadherins that connect these junctional complexes with the actin cytoskeleton as well as contribute to signaling networks (10-12). For numerous malignancies, including carcinoma of the esophagus, colon, stomach, and breast, loss of regular cadherin/catenin expression patterns had been correlated with tumor aggressiveness (13-15). In melanoma, these associations are less certain. Each of the three classic cadherin molecules have been evaluated as prognostic markers in multiple retrospective cohort studies of varying quality with mixed results. In multivariable analysis, decreased levels of P-cadherin (placental), a protein normally expressed in the basal layer of the epidermis, have been shown to be associated with faster disease progression in thin (<2 mm) lesions (16) but did not reach significance for all-cause mortality in another study (17). Gain of N-cadherin (neuronal) expression was significantly associated with increased all-cause mortality in one of two published univariate log-rank analyses and did not retain its significance in the one publication that included adjusted estimates (18, 19).

Only crude univariate data have been published for E-cadherin (epidermal) with one study showing improved survival with retained E-cadherin in the subset of patients with thin (<3.0 mm) superficial spreading melanomas (20) and a second showing no association for a cohort of nodular melanomas (19). Among the catenins, only β-catenin has been evaluated with respect to melanoma patient outcomes. Whereas two of three studies found a significant association ($P < 0.001$) between cytoplasmic β-catenin and improved survival on univariate analysis (19, 21, 22), this association was eliminated in the one study that simultaneously conducted multivariable analyses (22). Evaluation of the remaining catenins is limited to descriptive cross-sectional analyses across a progression series of benign melanocytic lesions, primary melanomas, and metastatic melanomas. In one series that included 13 benign nevi, 34 primary melanomas, and 20 metastatic melanomas, α-catenin expression has been shown to be more highly expressed in primaries compared with metastases and in thinner versus thicker lesions (23). This same study reported no association between either p120-catenin or γ-catenin with both Breslow thickness and tumor status (23). One other study attempted to investigate γ-catenin but could not detect this marker in their immunohistochemical assay (24).

To further elucidate the roles of E-cadherin, N-cadherin, and P-cadherin as well as the associated α-catenin, β-catenin, γ-catenin, and p120-catenin in the progression and prognosis of CMM, our goal was to determine whether any of these markers possessed independent prognostic significance for all-cause mortality in our cohort of 201 serial cases of primary melanoma when considered in a multivariable model adjusting for known clinicopathologic correlates of melanoma outcome using quantitative measures of protein expression for these candidates obtained using fluorescence-based immunohistochemistry on a tissue microarray. We also were interested in more extensively assessing the cross-sectional relationships both among the individual markers themselves as well as with relevant clinicopathologic features from the included specimens. Finally, to assess the interrelationships between adhesion marker expression patterns, we used hierarchical clustering to define discrete patient subpopulations and then assessed overall survival toward the goal of using a systems approach to understand the relationship between adhesion proteins and prognosis.

Materials and Methods

Patients and Specimens. A retrospective review of the Yale University Department of Pathology archives from 1959 to 1994 was conducted and 201 unique newly diagnosed cases of primary invasive melanoma for which both the surgical specimen was not exhausted during the diagnostic evaluation and documented clinical follow-up for a minimum of 10 years were identified. For 12 of these cases, multiple primary lesions were identified and blocks from each lesion were obtained. In addition, a series of 274 melanoma metastases was also retrieved. Clinical data describing patient demographics (age at diagnosis, calendar year of diagnosis, gender, and race) as well as clinical variables (histopathologic subtype and stage at diagnosis) were obtained following a medical record review. Where applicable, record of adjuvant or palliative therapy was also captured. This study was approved by the Yale University Human Investigations Committee (protocol 8219).

Formalin-fixed, paraffin-embedded specimens corresponding to the selected cases were retrieved. A single investigator (A.J.B.) reviewed a H&E section from each specimen to confirm the histologic diagnosis of malignant melanoma before inclusion on the tissue microarray and, for the primary cutaneous lesions, measured Breslow thickness, Clark level, microscopic satellites, tumor-infiltrating lymphocytes, and the presence of ulceration. A 0.6 mm tissue microarray was constructed according to published methods (25). Sections (5 μm) were cut from the tissue microarray master using a tissue microtome, transferred to glass slides using a UV cross-linkable tape transfer system (Instrumedics), dipped in paraffin, and stored in a nitrogen chamber to prevent antigen degeneration before staining (26).

Immunohistochemistry. Slides were deparaffinized using two xylene exchanges followed by rehydration through an ethanol gradient. Antigen retrieval was done by boiling the slides in a sealed pressure cooker containing 6.5 mmol/L sodium citrate (pH 6.0) for 15 min. Endogenous peroxidase activity was blocked with 0.75% hydrogen peroxide in absolute methanol at room temperature. Immunohistochemical staining was done by first incubating the slides with 0.3% bovine serum albumin dissolved in 1 mol/L TBS (pH 8.0) for 30 min at room temperature followed by application of a mouse antibody directed at one of the target proteins multiplexed with rabbit polyclonal anti-S100B (DAKO) 1:650 on each tissue microarray slide, the latter to distinguish the regions corresponding to melanoma from surrounding tissue in the absence of counterstain.

Target antibodies were as follows: α-catenin, mouse monoclonal clone CAT-7A4 (Zymed Laboratories) 1:150; β-catenin, mouse monoclonal clone 14 (BD Transduction Laboratories) 1:2500; p120-catenin, mouse monoclonal clone 98 (BD Transduction Laboratories) 1:400; γ-catenin, mouse monoclonal clone 15 (BD Transduction Laboratories) 1:50; N-cadherin, mouse monoclonal clone 3B9 (Zymed Laboratories) 1:150; E-cadherin, mouse monoclonal clone 36 (BD Transduction Laboratories) 1:400; and P-cadherin, mouse monoclonal clone 56 (BD Transduction Laboratories) 1:250. Primary antibodies were incubated at 4°C overnight. Validation of these primary antibodies has been reported previously by our laboratory (13, 27, 28). The secondary antibodies, Alexa 488–conjugated goat anti-rabbit (1:100; Molecular Probes) diluted into Envision anti-mouse (neat; DAKO) were applied for 1 h at room temperature. To visualize the nuclei, 4′,6-diamidino-2-phenylindole (1:100) was included with the secondary antibodies. Finally, a 10-min Cy5-tyramide (Perkin-Elmer Life Sciences) incubation labeled the target. Cores of formalin-fixed, paraffin-embedded melanoma cell line blocks (29), the expression status of which for each of the target proteins was determined previously by Western blot, served as internal positive and negative controls. Additional negative controls were obtained by omitting the target protein primary antibody.

Table 1. Distribution of clinicopathologic variables among the primary tumors

Variable	Females (n = 106), n (%)*	Males (n = 95), n (%)	P
Age at diagnosis (y)	57.82 ± 15.32	58.36 ± 16.01	0.81
Stage at diagnosis			
Localized	80 (81.6)	73 (84.9)	0.04 †
Nodal spread	11 (11.2)	2 (2.3)	
Distant disease	7 (7.1)	11 (12.8)	
Breslow thickness (mm)	2.41 ± 2.04	2.39 ± 1.88	0.95
Clark level			
II	18 (17.8)	21 (22.8)	0.22
III	40 (39.6)	35 (39.2)	
IV	27 (26.7)	30 (32.6)	
V	16 (15.8)	6 (6.5)	
Ulceration			
Yes	30 (30.6)	25 (28.4)	0.74
No	68 (69.4)	63 (71.6)	
Microsatellitosis			
Yes	26 (27.1)	16 (17.6)	0.12
No	70 (72.9)	75 (82.4)	
Histology			
Superficial spreading	69 (69.0)	56 (61.5)	0.14
Nodular	11 (11.0)	18 (18.7)	
Lentigo maligna melanoma	2 (2.0)	6 (6.6)	
Other	18 (18.0)	12 (13.2)	
Tumor-infiltrating lymphocytes			
None	7 (6.9)	7 (7.5)	0.99
Sparse	16 (15.8)	14 (15.1)	
Nonbrisk	55 (54.5)	52 (55.9)	
Brisk	23 (22.8)	20 (21.5)	
Anatomic site of primary			
Head/neck	10 (11.8)	16 (20.3)	0.0002 †
Trunk	16 (18.8)	35 (44.3)	
Upper extremity	16 (18.8)	9 (11.4)	
Lower extremity	43 (50.6)	19 (24.1)	
Received radiation therapy			
Yes	12 (11.7)	4 (4.3)	0.07
No	91 (88.4)	89 (95.7)	
Received chemotherapy			
Yes	13 (12.6)	10 (10.8)	0.68
No	90 (87.4)	83 (89.3)	
Received immunomodulators			
Yes	9 (8.7)	2 (2.2)	0.06
No	94 (91.3)	91 (97.9)	

*Numbers may not sum to total due to missing observations; percentages may not sum to 100% due to rounding.
† Significant at $P < 0.05$

Automated Image Acquisition and Analysis. The Automated Quantitative Analysis (AQUA) image acquisition and analysis was done as described previously (30). Sets of monochromatic, high-resolution (1024 × 1024, 0.5 μm) images are captured for each histospot for each of the 4′,6-diamidino-2-phenylindole, Alexa 488, and Cy5 fluorescent channels using a modified computer-controlled epifluorescence microscope (Olympus BX-51 with xy stage and z controller) illuminated by a high-pressure mercury bulb (Photonic Solutions) with a high-resolution monochromatic camera (Cooke). Two images are captured for each channel: one in the plane of focus and one 8 μm below it. Compartmentalization of each histospot and quantitation of the target protein signal within each compartment are executed as follows. The Alexa 488 signal representing S100B staining is binary gated to indicate whether a pixel is within the tumor mask (''on'') or not (''off''). Within the region defined by the tumor, the nuclear compartment is defined by applying the rapid exponential subtraction algorithm to the 4′,6-diamidino-2-phenylindole channel images, which restricts the nuclear compartment assignment to only those pixels that show any positive 4′,6-diamidino-2-phenylindole signal within the plane of focus. The nonnuclear compartment is then defined by the Pixel-Based Locale Assignment for Compartmentalization of Expression algorithm as all pixels assigned to the tumor mask but are not included within the nuclear compartment.

Finally, target antigen expression levels were determined in an automated fashion, blinded to any *a priori* clinical information, following application of the rapid exponential subtraction algorithm to the Cy5 images to obtain a relative pixel intensity restricted to the signal emanating from the plane of focus. The final AQUA score for the entire tumor mask or any of its subcellular compartments is calculated as the average AQUA score for each of the individual pixels included in the selected compartment and is reported on a scale of 0 to 4095.

Statistical Analysis. Histospots containing less than 0.17 mm^2 of tumor were excluded from further analysis. For the set of 12 individuals represented by multiple primary lesions, a mean AQUA score for each marker based on the available raw data was calculated and incorporated in all subsequent analyses described below. Bivariate comparisons between individual target antigens or between target antigens and clinicopathologic variables were assessed using the Spearman rank correlation, ANOVA, or χ^2 analysis as appropriate.

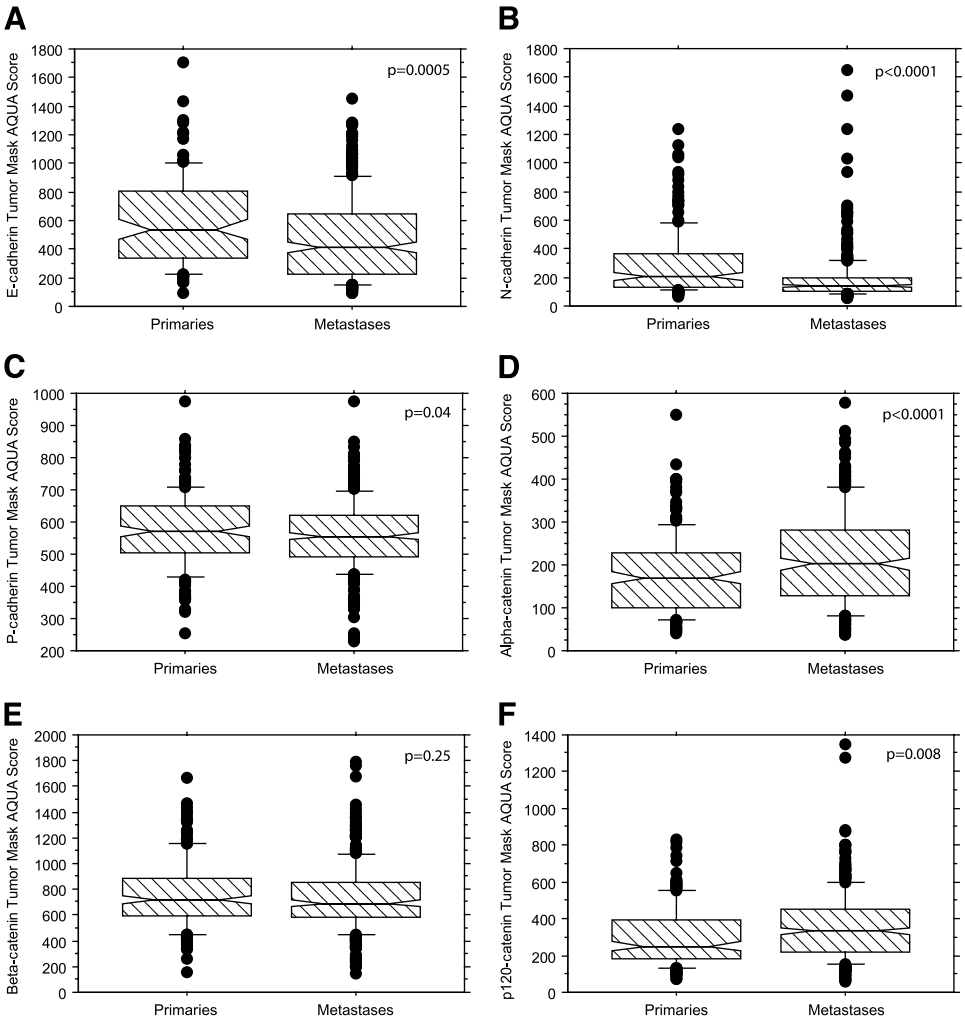

Figure 1. Box-and-whisker plots comparing the distributions of the composite AQUA score for the entire area under the tumor mask between the primary and metastatic lesions for each of the assayed adhesion markers. Presented *P* values were determined from an ANOVA.

Table 2. Univariate and multivariable all-cause mortality HRs for the adhesion marker tertiles in the primary melanoma cases

Adhesion marker	Univariate HR (95% CI)	*P*	Multivariable HR (95% CI)*	*P*
E-cadherin				
Tertile 1 (AQUA score 0-422)	1.00		1.00	
Tertile 2 (AQUA score 423-738)	0.68 (0.41-1.12)	0.13	0.59 (0.32-1.08)	0.09
Tertile 3 (AQUA score 739-1,433)	0.62 (0.37-1.03)	0.06	0.57 (0.29-1.12)	0.10
N-cadherin				
Tertile 1 (AQUA score 0-156)	1.00		1.00	
Tertile 2 (AQUA score 157-301)	0.72 (0.46-1.11)	0.13	0.84 (0.50-1.43)	0.52
Tertile 3 (AQUA score 302-1,233)	0.54 (0.34-0.85)	**0.008**	0.91 (0.52-1.58)	0.72
P-cadherin				
Tertile 1 (AQUA score 0-531)	1.00		1.00	
Tertile 2 (AQUA score 532-608)	1.15 (0.73-1.81)	0.54	0.96 (0.56-1.65)	0.89
Tertile 3 (AQUA score 609-974)	1.18 (0.74-1.86)	0.49	1.07 (0.63-1.84)	0.80
α-Catenin				
Tertile 1 (AQUA score 0-116)	1.00		1.00	
Tertile 2 (AQUA score 117-201)	0.95 (0.62-1.46)	0.81	0.86 (0.52-1.42)	0.56
Tertile 3 (AQUA score 202-549)	1.07 (0.70-1.63)	0.77	1.02 (0.63-1.65)	0.94
β-catenin				
Tertile 1 (AQUA score 0-651)	1.00		1.00	
Tertile 2 (AQUA score 652-813)	0.92 (0.59-1.43)	0.72	0.70 (0.41-1.18)	0.18
Tertile 3 (AQUA score 814-1,665)	0.82 (0.53-1.28)	0.38	0.82 (0.49-1.38)	0.45
p120-catenin				
Tertile 1 (AQUA score 0-209)	1.00		1.00	
Tertile 2 (AQUA score 210-348)	0.89 (0.55-1.44)	0.63	0.70 (0.40-1.23)	0.22
Tertile 3 (AQUA score 349-831)	0.99 (0.62-1.58)	0.97	0.82 (0.48-1.40)	0.46

*Multivariable HRs are adjusted for age at diagnosis, gender, stage at diagnosis, Breslow thickness (mm), presence of ulceration and receipt of any cytotoxic chemotherapy during the course of disease.

Hierarchical clustering of target antigen expression profiles using the average-linked clustering algorithm was executed on the Cluster/TreeView software package (31) for the subset of individuals with valid AQUA scores for ≥5 of the target antigens (n = 355) following log transformation for normalization of the AQUA scores within each target. Survival curves were calculated using the Kaplan-Meier product-limit method and significance determined by the Mantel-Cox log-rank statistic. Crude and multivariable hazard ratios (HR) were determined using Cox proportional hazards modeling. All statistical analyses were done using Statview or SAS version 9.1.3 (SAS Institute).

Results

Patient Characteristics. Our cohort of 201 primary melanomas included 106 females and 95 males (Table 1). Overall, more than 50% of the cohort had T_1-T_2 lesions (thinner than 2.0 mm) but with Clark levels of invasion between II and IV, localized lesions at the time of diagnosis, superficial spreading melanomas, and nonulcerated lesions. The mean age at diagnosis was 58 years. Twelve percent of all participants received any therapeutic intervention other than surgery. For those individuals who did not die during follow-up, the median recorded follow-up time was 17.0 years, with only 25% of the individuals possessing follow-up time of <9.1 years. Only the location of the primary tumor was markedly different between genders, with men more likely to have melanomas on the head/neck and upper extremities and women more likely to present with lesions on the lower extremities.

Clinicopathologic Associations. Quantitative analysis of expression was done for the panel of adhesion markers as described. The differential distribution of AQUA scores between the primary and metastatic specimens is presented (Fig. 1). E-cadherin (P = 0.0005), N-cadherin (P < 0.0001), and P-cadherin (P = 0.04) were all significantly down-regulated and α-catenin (P < 0.0001) and p120-catenin (P = 0.008) were up-regulated across the metastatic specimens compared with the primary lesions. No significant difference between primary and metastatic lesion was observed for β-catenin (P = 0.25). γ-catenin expression was not detected using the AQUA platform and was dropped from further analysis.

We next evaluated the correlations between all pairwise combinations of the adhesion markers across the entire set of 475 unique specimens. Positive associations were noted for the relationships between P-cadherin and β-catenin (r_s = 0.54; P < 0.0001), P-cadherin and p120-catenin (r_s = 0.38; P < 0.0001), α-catenin and β-catenin (r_s = 0.26; P < 0.0001), and β-catenin and p120-catenin (r_s = 0.47; P < 0.0001), with negative correlations noted between E-cadherin and P-cadherin (r_s = −0.15; P = 0.004). The associations between α-catenin and each of P-cadherin and p120-catenin as well as the association between N-cadherin and p120-catenin were modified by lesion type. A positive relationship was observed between α-catenin and P-cadherin among the primaries (r_s = 0.23; P = 0.005); no association was found among the metastases (r_s = −0.07; P = 0.24). Positive associations of different magnitude were noted between α-catenin and p120-catenin between the primaries (r_s = 0.48; P < 0.0001) and the metastases (r_s = 0.31; P < 0.0001). A negative association was noted among the metastases between N-cadherin and p120-catenin (r_s = −0.23; P = 0.0002) but not among the primaries (r_s = 0.09; P = 0.30).

Measures of association were also obtained between each of the adhesion markers and gender, Breslow

thickness, presence of ulceration, histopathologic subtype, stage at diagnosis, anatomic location of the primary lesion, and whether the participant received chemotherapy during the course of his/her disease for the set of primary tumors. Decreased levels of E-cadherin ($r_s = -0.22$; $P = 0.02$), N-cadherin ($r_s = -0.28$; $P = 0.0002$), and α-catenin ($r_s = -0.23$; $P = 0.002$) were observed with increasing Breslow thickness. Higher AQUA scores for p120-catenin were noted among the subset of lentigo maligna melanoma samples ($P = 0.008$) and higher N-cadherin AQUA scores were noted among truncal lesions ($P = 0.008$). Decreased levels of E-cadherin were also noted among the small subset ($n = 23$) who received chemotherapy compared with those who did not ($r_s = -0.26$; $P = 0.006$). No other significant relationships between adhesion marker AQUA scores and clinicopathologic variables were noted.

Individual Marker AQUA Scores and Relationship with Prognosis. The set of primary tumors were divided into tertiles according to the AQUA scores for each adhesion marker and Cox proportional hazards modeling was executed to determine both the crude and the adjusted all-cause mortality HRs for the middle and upper tertiles compared with the lowest tertile (Table 2). On univariate analysis, increasing levels of N-cadherin expression improved survival [tertile 2: HR, 0.72; 95% confidence interval (95% CI), 0.46-1.11; tertile 3: HR, 0.54; 95% CI, 0.34-0.85] with an overall significant log-rank score of 7.31 ($P = 0.03$; Fig. 2A). This association, however, did not retain its significance in the multivariable analysis following adjustment for age at diagnosis, gender, stage at diagnosis, Breslow thickness (mm), presence of ulceration, and receipt of chemotherapy. We also noted a trend towards significance among the E-cadherin tertiles where higher expression levels suggested improved survival (log-rank score = 4.04; $P = 0.13$; Fig. 2B). This association maintained its marginal trend towards significance even after adjusting for the independent clinical covariates (tertile 2: adjusted HR, 0.59; 95% CI, 0.32-1.08; tertile 3: adjusted HR, 0.57; 95% CI, 0.29-1.12). Neither the crude nor the adjusted estimates for P-cadherin, α-catenin, β-catenin, and p120-catenin reached statistical significance.

Hierarchical Clustering of Adhesion Markers Defines Subclasses of Melanoma. Hierarchical clustering on the subset of samples with valid AQUA scores for five of the six target antigens ($n = 355$) introduced four distinctive clusters (Fig. 3A). Cluster 1 ($n = 162$) is characterized by high expression of α-catenin and E-cadherin concurrent with low N-cadherin expression. Cluster 2 ($n = 33$) is defined by low expression of α-catenin and E-cadherin but high levels of P-cadherin, β-catenin, and p120-catenin and modest N-cadherin. Cluster 3 ($n = 126$) contains low to average expression of all six markers and cluster 4 ($n = 36$) is denoted by high levels of N-cadherin in concert with modest levels of E-cadherin. Distribution of cluster assignments significantly differed between primary ($n = 125$) and metastatic samples ($n = 230$; $\chi^2_{df=3} = 8.02$; $P = 0.046$) with clusters 2 and 4 occurring disproportionately among the primary tumors (12.0% and 14.4% in primaries versus 7.8% and 7.0% in the metastases, respectively) and cluster 1 was more frequent among the metastatic samples (39.2% in primaries versus 49.1% in metastases).

Among the primary tumors, cluster assignment was only associated with ulceration where higher percentages of ulcerated lesions were assigned to clusters 2 and 4 (20.5% and 23.1% among ulcerated primaries versus 8.0% and 12.0% among nonulcerated primaries). No association was found between cluster assignment and age at diagnosis ($P = 0.53$), Breslow thickness ($P = 0.24$), gender ($P = 0.09$), stage at diagnosis ($P = 0.39$), anatomic site of the primary ($P = 0.68$), histologic subtype ($P = 0.81$), or receipt of cytotoxic chemotherapy ($P = 0.17$).

Product-limit survival analysis for all-cause mortality according to cluster assignment revealed a significant association (log-rank = 10.54; $P = 0.01$) with cluster 4 showing the most favorable trajectory and cluster 2 the least favorable (Fig. 3B). To further explore these relationships, univariate and multivariable Cox proportional hazards modeling, the latter adjusting for age at

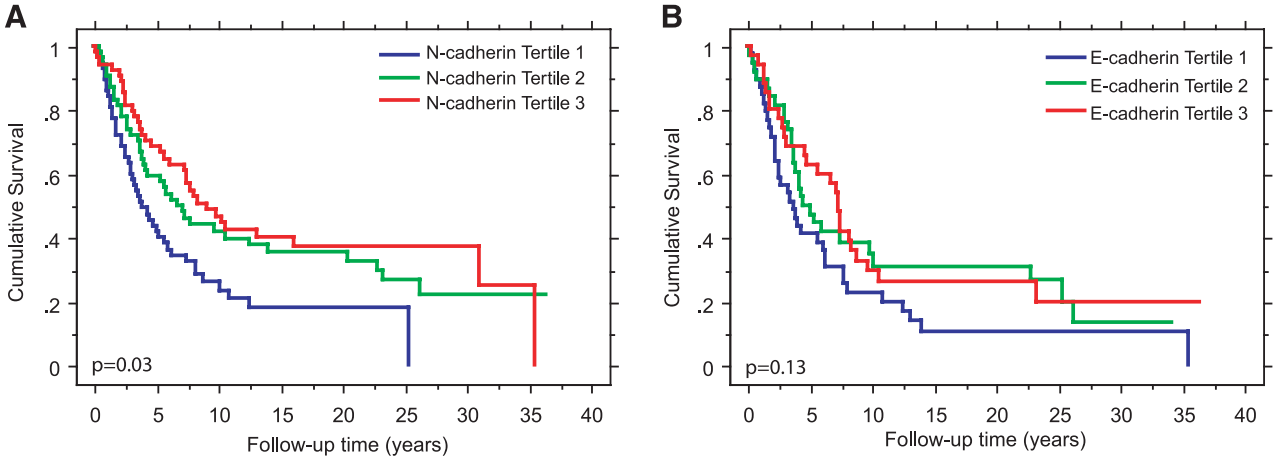

Figure 2. Kaplan-Meier product-limit survival curves describing the association between all-cause mortality and (**A**) E-cadherin or (**B**) N-cadherin according to tertile of protein expression among the subset of individuals with primary tumors that yielded valid AQUA scores for the respective markers (E-cadherin eligible $n = 116$, N-cadherin eligible $n = 170$).

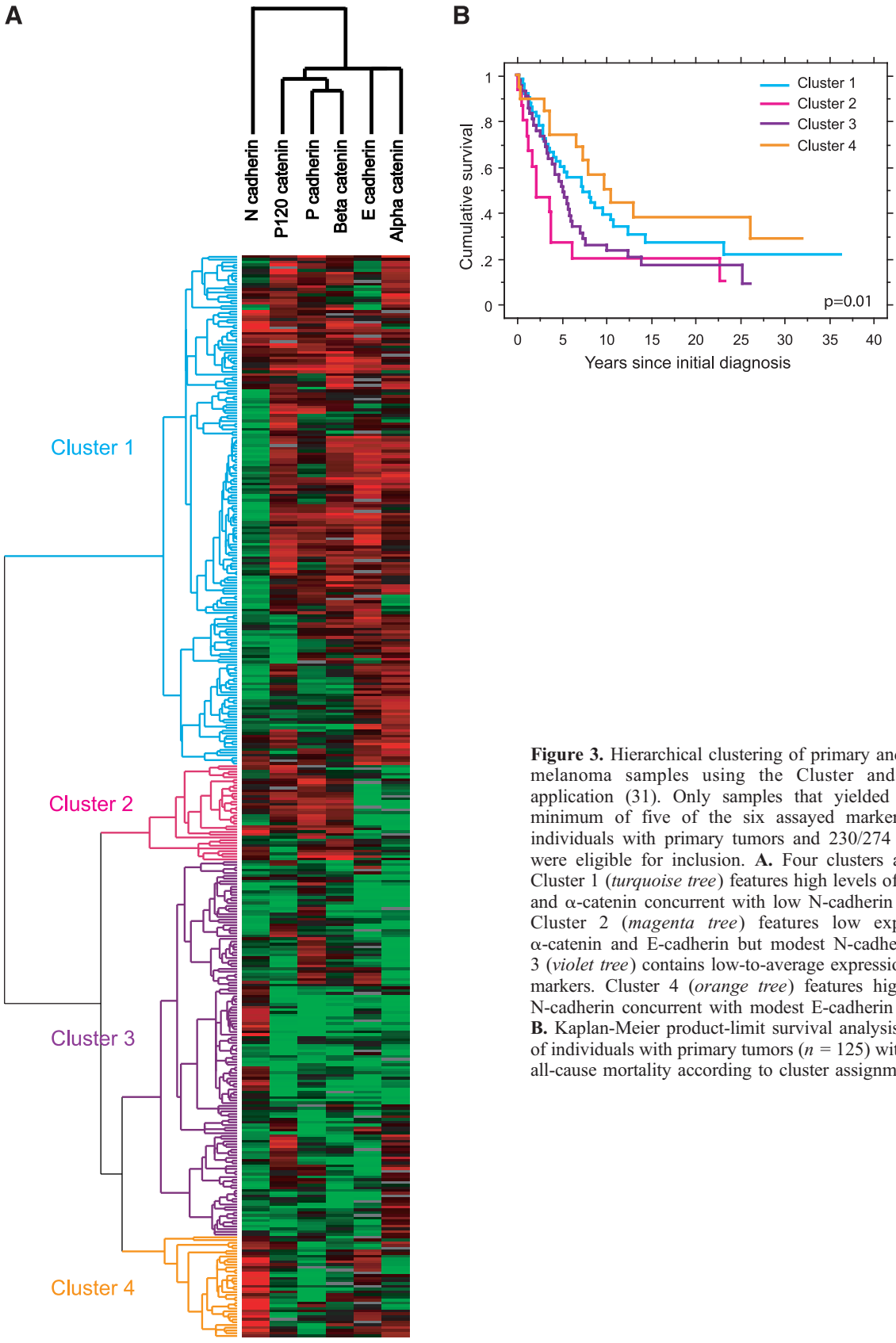

Figure 3. Hierarchical clustering of primary and metastatic melanoma samples using the Cluster and TreeView application (31). Only samples that yielded data for a minimum of five of the six assayed markers (125/201 individuals with primary tumors and 230/274 metastases) were eligible for inclusion. **A.** Four clusters are defined. Cluster 1 (*turquoise tree*) features high levels of E-cadherin and α-catenin concurrent with low N-cadherin expression. Cluster 2 (*magenta tree*) features low expression of α-catenin and E-cadherin but modest N-cadherin. Cluster 3 (*violet tree*) contains low-to-average expression of all six markers. Cluster 4 (*orange tree*) features high levels of N-cadherin concurrent with modest E-cadherin expression. **B.** Kaplan-Meier product-limit survival analysis for the set of individuals with primary tumors (n = 125) with respect to all-cause mortality according to cluster assignment.

diagnosis, gender, stage at diagnosis, presence of ulceration, Breslow thickness (mm), and receipt of chemotherapy, was conducted for the four cluster assignments using cluster 1 as the reference group. Each of the clinical predictors was significant in univariate modeling. Compared with the reference cluster, cluster 2 showed a significantly increased crude risk of death (crude HR, 2.15; 95% CI, 1.13-4.13; $P = 0.02$), a relationship that strengthened in multivariable analysis (adjusted HR, 3.29; 95% CI, 1.50-7.19; $P = 0.003$). None of the other clusters significantly differed from the reference in the adjusted analysis. Additionally, age at diagnosis ($P < 0.0001$), receipt of chemotherapy ($P = 0.0004$), and stage at diagnosis ($P = 0.0005$ for distant disease) remained significant independent predictors of outcome (Table 3).

Discussion

The high case fatality rate of metastatic melanoma has prompted not only the identification of molecular changes necessary to stimulate invasion and metastasis in melanoma but also the evaluation of their expression in primary tumors as independent prognostic markers orthogonal to the commonly assayed clinical variables. EMT, the process that describes the transition of epithelially derived cancer cells into a mesenchymal phenotype with concomitant loss of adhesion to the tumor mass, is considered to be the first necessary step for tumor invasion and metastasis. Mature melanocytes, although derived from the neural crest, reside in the basal layer of the epidermis where they establish heterotypic cell-cell interactions with basal keratinocytes through the mediation of E-cadherin (32). P-cadherin is also expressed in normal melanocytes and also likely plays a role in regulating regular cell-cell interactions between melanocytes and their surrounding cells (33). The down-regulation of either E-cadherin or P-cadherin, or the induction of N-cadherin, facilitates melanoma cell migration and invasion in *in vitro* assays (34-36). In this analysis, we report on the relevance of protein expression levels for E-cadherin, P-cadherin, and N-cadherin and for α-catenin, β-catenin, and p120-catenin, intracellular signal transducers of these cadherins to both melanoma progression and prognosis.

Although this is the first time quantitative assessments of associations have been examined in melanoma, our cross-sectional results are consistent with previously known interactions among the cadherins and catenins. In accordance with data published by Sanders et al. (24), we have shown that P-cadherin and β-catenin have extremely similar expression profiles through Spearman correlation coefficients and a dendrogram after hierarchical clustering. According to our data, p120-catenin and α-catenin also share similarity to the former proteins. The high, positive r_s values among these pairwise combinations further strengthen the argument, with the association between α-catenin and P-cadherin only being significant among the primary tumors. These findings are also consistent with the known binding of α-catenin to β-catenin (37). Our inability to resolve γ-catenin expression above the limit of detection for the AQUA platform is consistent with very weak to absent expression in melanocytic lesions as reported by others (38).

Consistent with previous publications (16, 19), we showed lower mean levels of E-cadherin and P-cadherin among the metastatic lesions compared with the primary melanomas and no significant difference among β-catenin levels. We also show significant negative trends of E-cadherin and α-catenin with Breslow thickness, recapitulating previously reported data (19, 23). Although our analysis did not reveal a significant association between Breslow thickness and P-cadherin expression levels, these data are supported by the literature. First, both of the published studies evaluating P-cadherin discriminated between cytoplasmic and membranous staining, whereas ours did not. Next, although both studies reported larger proportions of thinner lesions having increased levels of membranous staining, the association between cytoplasmic staining and tumor thickness is uncertain, with one report suggesting

Table 3. Crude and multivariable all-cause mortality HRs for clinicopathologic covariates and the adhesion molecule classification clusters among the subjects with primary invasive melanoma

Variable	Crude association (95% CI)	*P*	Multivariable model (95% CI)	*P*
Breslow thickness (per unit mm)	1.29 (1.19-1.40)	<0.0001	1.12 (0.97-1.30)	0.13
Gender				
Male	1.00		1.00	
Female	0.71 (0.51-1.00)	0.05	0.96 (0.58-1.60)	0.88
Mean age at diagnosis (per year)	1.03 (1.02-1.04)	<0.0001	1.04 (1.02-1.06)	<0.0001
Stage at diagnosis				
Localized to skin	1.00		1.00	
Present in lymph nodes	2.55 (1.40-4.64)	0.002	1.32 (0.55-3.15)	0.53
Spread to distant sites	4.15 (2.48-6.97)	<0.0001	5.36 (2.07-13.88)	0.0005
Ulceration				
No	1.00		1.00	
Yes	1.47 (1.02-2.12)	0.04	1.49 (0.85-2.59)	0.16
Received any cytotoxic chemotherapy				
No	1.00		1.00	
Yes	2.38 (1.47-3.84)	0.0004	3.80 (1.82-7.90)	0.0004
Adhesion molecule cluster assignment				
Cluster 1	1.00		1.00	
Cluster 2	2.15 (1.13-4.13)	0.02	3.29 (1.50-7.19)	0.003
Cluster 3	1.44 (0.88-2.34)	0.14	1.45 (0.80-2.63)	0.22
Cluster 4	0.67 (0.34-1.34)	0.26	0.77 (0.34-1.74)	0.52

increased cytoplasmic staining and the other presenting decreased cytoplasmic staining with thicker lesions (16, 19). In this setting, a true null result, which our data support, cannot be ruled out.

None of the assayed adhesion markers showed an independent relationship with all-cause mortality among the assayed primary tumors; the protective effect for increased E-cadherin expression trended toward but did not achieve statistical significance and the crude, apparently paradoxical, protective effect for increased N-cadherin expression was not sustained following adjustment for known clinicapathologic factors. Yet, our cluster analysis introduces four broad subclasses of melanoma that can be distinguished by their overall survival. Importantly, cluster 2, which shows down-regulation of E-cadherin and α-catenin in the setting of modest N-cadherin and high β-catenin expression, yields a 3.29-fold increased risk of death (95% CI, 1.50-7.19) even after adjusting for known clinicopathologic factors. Consistent with the expected phenotype following a successful EMT, cluster 2 corroborates the recent publications by two groups describing worse outcomes among the subset of melanomas who successfully completed an EMT as evidenced by the simultaneous down-regulation of proteins promoting keratinocyte adhesion (e.g., E-cadherin and P-cadherin) and up-regulation of proteins that facilitate interactions with and invasion through stroma (e.g., N-cadherin and osteonectin/SPARC; refs. 18, 39). Furthermore, the high β-catenin in the setting of low E-cadherin may promote preferential activity of the Wnt signaling cascade (12), another marker associated previously with poor outcome in melanoma (21, 22).

A second subclass, cluster 1, shows high levels of all of the cadherin-catenin proteins consistent with an epithelioid type of melanoma. Finally, cluster 4 is defined by high N-cadherin expression concurrent with modest E-cadherin expression. Unexpectedly, despite that cluster 4 melanomas expressed the highest levels of N-cadherin among our entire cohort, this group displayed the best survival on univariate analysis with the failure to reach statistical significance driven by both the arbitrary choice of cluster 1 as the reference group and the small number of tumors in this cluster. In this group, especially as E-cadherin continues to be expressed, the high level of N-cadherin expression is not a harbinger of the EMT but rather a nod to a key phase in melanoblast development from the neural crest. During embryonic development, nascent neural crest cells express N-cadherin to form the adherens junctions required for connections with other neural tube cells. Consequently, the EMT associated with the migration of neural crest cells requires the initial ''decrease'' of N-cadherin expression to facilitate egress from the dorsal surface of the neural tube (40). Thus, very high levels of N-cadherin may recapitulate a very early but noninvasive, developmental phenotype.

These findings confirm and extend the cDNA-based findings of both Bittner et al. (4) and Onken et al. (41) in the proteomic-based classification of epithelioid and neural crest classes of melanoma. More importantly, our classification scheme has differentiated two classes of melanomas that express N-cadherin: the EMT-positive type and the well-differentiated neural crest precursor type.

Strengths of our study included the use of automated quantitative assessment of protein expression that eliminates potential information bias from the traditional subjective categorical assessment of immunohistochemical results by pathologists. We also note several limitations to our study. First, our use of hierarchical clustering as the discriminator of our melanoma subclasses limits our ability to classify new samples given a vector of AQUA scores for those samples. As there is no mathematically grounded method of estimating the error associated with a clustering run and new samples can only be placed in the hierarchy following re-clustering run, which might rearrange the contents of the previous clusters, we would need to translate our clustering results to a more robust analytic platform before advancing a diagnostic based on the findings reported here. Next, although our cohort is one of the larger cohorts reported in the literature, our cohort still contains a limited number of samples, especially among the two groups of interest. Additionally, our cohort was collected retrospectively and includes cases that span a 35-year period of accrual where large secular shifts in the diagnosis and management of CMM occurred. Although our cohort is useful for understanding the effect of molecular markers on CMM natural history, it will be essential that this result be validated on a prospectively collected CMM cohort that were subjected to current standards of care. Future efforts will also be required to integrate these classes with the newer classes defined by the molecular classification studies of Bastian et al. (42).

In summary, this analysis of cadherin-based adhesion molecules in the behavior of melanoma reveals differences between neural crest–derived melanoma and other common epithelial-derived solid tumors with respect to cadherin-catenin shifts during tumor progression. Specifically, unlike epithelial tumors where N-cadherin overexpression exclusively suggests an EMT that facilitates metastatic behavior, N-cadherin overexpression in melanoma can describe either an EMT-positive, metastasis-prone, or a well-differentiated tumor. Evaluation of additional cadherins that can further distinguish between these dichotomous N-cadherin-positive states is needed.

References

1. Jemal A, Siegel R, Ward E, Murray T, Xu J, Thun MJ. Cancer statistics, 2007. CA Cancer J Clin 2007;57:43–66.
2. Balch CM, Soong SJ, Gershenwald JE, et al. Prognostic factors analysis of 17,600 melanoma patients: validation of the American Joint Committee on Cancer melanoma staging system. J Clin Oncol 2001;19:3622–34.
3. Gimotty PA, Elder DE, Fraker DL, et al. Identification of high-risk patients among those diagnosed with thin cutaneous melanomas. J Clin Oncol 2007;25:1129–34.
4. Bittner M, Meltzer P, Chen Y, et al. Molecular classification of cutaneous malignant melanoma by gene expression profiling. Nature 2000;406:536–40.
5. Winnepenninckx V, Lazar V, Michiels S, et al. Gene expression profiling of primary cutaneous melanoma and clinical outcome. J Natl Cancer Inst 2006;98:472–82.
6. Golub TR, Slonim DK, Tamayo P, et al. Molecular classification of cancer: class discovery and class prediction by gene expression monitoring. Science 1999;286:531–7.
7. van't Veer LJ, Dai H, van de Vijver MJ, et al. Gene expression profiling predicts clinical outcome of breast cancer. Nature 2002;415:530–6.
8. Guarino M, Rubino B, Ballabio G. The role of epithelial-mesenchymal transition in cancer pathology. Pathology 2007;39:305–18.

9. Tucker RP. Neural crest cells: a model for invasive behavior. Int J Biochem Cell Biol 2004;36:173–7.
10. Halbleib JM, Nelson WJ. Cadherins in development: cell adhesion, sorting, and tissue morphogenesis. Genes Dev 2006;20:3199–214.
11. Huber MA, Kraut N, Beug H. Molecular requirements for epithelial-mesenchymal transition during tumor progression. Curr Opin Cell Biol 2005;17:548–58.
12. Luo J, Chen J, Deng ZL, et al. Wnt signaling and human diseases: what are the therapeutic implications? Lab Invest 2007;87:97–103.
13. Dolled-Filhart M, McCabe A, Giltnane J, Cregger M, Camp RL, Rimm DL. Quantitative *in situ* analysis of β-catenin expression in breast cancer shows decreased expression is associated with poor outcome. Cancer Res 2006;66:5487–94.
14. Gould Rothberg BE, Bracken MB. E-cadherin immunohistochemical expression as a prognostic factor in infiltrating ductal carcinoma of the breast: a systematic review and meta-analysis. Breast Cancer Res Treat 2006. Epub: DOI 10.1007/s10549-006-9248-2.
15. Takayama T, Shiozaki H, Shibamoto S, et al. β-Catenin expression in human cancers. Am J Pathol 1996;148:39–46.
16. Bauer R, Wild PJ, Meyer S, et al. Prognostic relevance of P-cadherin expression in melanocytic skin tumours analysed by high-throughput tissue microarrays. J Clin Pathol 2006;59:699–705. Epub 2006 Mar 24.
17. Pacifico MD, Grover R, Richman PI, Buffa F, Daley FM, Wilson GD. Identification of P-cadherin in primary melanoma using a tissue microarrayer: prognostic implications in a patient cohort with long-term follow up. Ann Plast Surg 2005;55:316–20.
18. Alonso SR, Tracey L, Ortiz P, et al. A high-throughput study in melanoma identifies epithelial-mesenchymal transition as a major determinant of metastasis. Cancer Res 2007;67:3450–60.
19. Bachmann IM, Straume O, Puntervoll HE, Kalvenes MB, Akslen LA. Importance of P-cadherin, β-catenin, and Wnt5a/frizzled for progression of melanocytic tumors and prognosis in cutaneous melanoma. Clin Cancer Res 2005;11:8606–14.
20. Andersen K, Nesland JM, Holm R, Florenes VA, Fodstad O, Maelandsmo GM. Expression of S100A4 combined with reduced E-cadherin expression predicts patient outcome in malignant melanoma. Mod Pathol 2004;17:990–7.
21. Kielhorn E, Provost E, Olsen D, et al. Tissue microarray-based analysis shows phospho-β-catenin expression in malignant melanoma is associated with poor outcome. Int J Cancer 2003;103:652–6.
22. Maelandsmo GM, Holm R, Nesland JM, Fodstad O, Florenes VA. Reduced β-catenin expression in the cytoplasm of advanced-stage superficial spreading malignant melanoma. Clin Cancer Res 2003;9:3383–8.
23. Zhang XD, Hersey P. Expression of catenins and p120cas in melanocytic nevi and cutaneous melanoma: deficient α-catenin expression is associated with melanoma progression. Pathology 1999;31:239–46.
24. Sanders DS, Blessing K, Hassan GA, Bruton R, Marsden JR, Jankowski J. Alterations in cadherin and catenin expression during the biological progression of melanocytic tumours. Mol Pathol 1999;52:151–7.
25. Kononen J, Bubendorf L, Kallioniemi A, et al. Tissue microarrays for high-throughput molecular profiling of tumor specimens. Nat Med 1998;4:844–7.
26. DiVito KA, Charette LA, Rimm DL, Camp RL. Long-term preservation of antigenicity on tissue microarrays. Lab Invest 2004;84:1071–8.
27. Dillon DA, D'Aquila T, Reynolds AB, Fearon ER, Rimm DL. The expression of p120ctn protein in breast cancer is independent of α- and β-catenin and E-cadherin. Am J Pathol 1998;152:75–82.
28. Reyes-Mugica M, Meyerhardt JA, Rzasa J, et al. Truncated DCC reduces N-cadherin/catenin expression and calcium-dependent cell adhesion in neuroblastoma cells. Lab Invest 2001;81:201–10.
29. Hoek K, Rimm DL, Williams KR, et al. Expression profiling reveals novel pathways in the transformation of melanocytes to melanomas. Cancer Res 2004;64:5270–82.
30. Camp RL, Chung GG, Rimm DL. Automated subcellular localization and quantification of protein expression in tissue microarrays. Nat Med 2002;8:1323–7. Epub 2002 Oct 21.
31. Eisen MB, Spellman PT, Brown PO, Botstein D. Cluster analysis and display of genome-wide expression patterns. Proc Natl Acad Sci U S A 1998;95:14863–8.
32. Haass NK, Smalley KS, Li L, Herlyn M. Adhesion, migration and communication in melanocytes and melanoma. Pigment Cell Res 2005;18:150–9.
33. Bauer R, Bosserhoff AK. Functional implication of truncated P-cadherin expression in malignant melanoma. Exp Mol Pathol 2006;81:224–30.
34. Hsu MY, Meier FE, Nesbit M, et al. E-cadherin expression in melanoma cells restores keratinocyte-mediated growth control and down-regulates expression of invasion-related adhesion receptors. Am J Pathol 2000;156:1515–25.
35. Li G, Satyamoorthy K, Herlyn M. N-cadherin-mediated intercellular interactions promote survival and migration of melanoma cells. Cancer Res 2001;61:3819–25.
36. Van Marck V, Stove C, Van Den Bossche K, et al. P-cadherin promotes cell-cell adhesion and counteracts invasion in human melanoma. Cancer Res 2005;65:8774–83.
37. Weis WI, Nelson WJ. Re-solving the cadherin-catenin-actin conundrum. J Biol Chem 2006;281:35593–7.
38. Krengel S, Groteluschen F, Bartsch S, Tronnier M. Cadherin expression pattern in melanocytic tumors more likely depends on the melanocyte environment than on tumor cell progression. J Cutan Pathol 2004;31:1–7.
39. Shields JM, Thomas NE, Cregger M, et al. Lack of extracellular signal-regulated kinase mitogen-activated protein kinase signaling shows a new type of melanoma. Cancer Res 2007;67:1502–12.
40. Bronner-Fraser M. Neural crest cell migration in the developing embryo. Trends Cell Biol 1993;3:392–7.
41. Onken MD, Ehlers JP, Worley LA, Makita J, Yokota Y, Harbour JW. Functional gene expression analysis uncovers phenotypic switch in aggressive uveal melanomas. Cancer Res 2006;66:4602–9.
42. Bastian BC, Olshen AB, LeBoit PE, Pinkel D. Classifying melanocytic tumors based on DNA copy number changes. Am J Pathol 2003;163:1765–70.